

PROFESSOR FERNANDA BORGES (Orcid ID : 0000-0003-1050-2402)

Article type : Research Article

Coumarins and adenosine receptors: new perceptions in structure-affinity relationships

André Fonseca^{a, b}, Maria João Matos^{*a}, Santiago Vilar^{a, b}, Sonja Kachler^c, Karl-Norbert Klotz^c, Eugenio Uriarte^{b, d} and Fernanda Borges^{*a}

^aCIQUP/Department of Chemistry and Biochemistry, Faculty of Sciences, University of Porto, 4169-007, Porto, Portugal

^bDepartamento Química Orgánica, Facultad de Farmacia, Universidad Santiago de Compostela, 15782, Santiago de Compostela, Spain

^cPharmacology and Toxicology Institute, University of Würzburg, 97078, Würzburg, Germany

^dInstituto de Ciencias Químicas Aplicadas, Universidad Autónoma de Chile, 7500912, Santiago de Chile, Chile.

*Corresponding Authors: Fernanda Borges, CIQUP/Department of Chemistry and Biochemistry, Faculty of Sciences, University of Porto, 4169-007, Porto, Portugal. E-mail: fborges@fc.up.pt

Maria João Matos, Organic Chemistry Department, Faculty of Pharmacy, University of Santiago de Compostela, 15782, Santiago de Compostela, Spain. Email: mariacmatos@gmail.com

Keywords: Coumarins; Adenosine Receptors; Carboxamidocoumarin;

This article has been accepted for publication and undergone full peer review but has not been through the copyediting, typesetting, pagination and proofreading process, which may lead to differences between this version and the Version of Record. Please cite this article as doi: 10.1111/cbdd.13075

This article is protected by copyright. All rights reserved.

Abstract

Adenosine receptors (ARs) subtypes are involved in several physiological and pharmacological processes. Ligands able to selectively modulate one receptor subtype can delay or slow down the progression of diverse diseases. In this context, our research group focused its investigation into the discovery and development of novel, potent and selective ARs ligands based on coumarin scaffold. Therefore, a series 3-phenylcarboxamidocoumarins were synthesised and their affinity for the human ARs subtypes was screened by radioligand binding assays for A_1 , A_{2A} and A_3 receptors and for A_{2B} by adenylyl cyclase assay. Compound **26** was found to be the most remarkable, with a hA_1/hA_3 and hA_{2A}/hA_3 selectivity of 42, for the A_3 AR ($K_i = 2.4 \mu\text{M}$). Receptor-driven molecular modelling studies have provided valuable information on the binding/selectivity data of compound **26** and for the following optimization process. Moreover, compound **26** present drug-like properties according to the general guidelines linked to the concept.

Introduction

Adenosine is an endogenous purine nucleoside with an important role in a diversity of biochemical processes, namely in energy transfer (adenosine triphosphate or ATP) and in cellular signalling (cyclic AMP). In the 1920's it was demonstrated for the first time adenosine biologic action in the cardiovascular system.¹ In addition to its clinical role as anti-arrhythmic agent, adenosine has been implicated in diverse pharmacological areas and throughout the years adenosine signaling pathways have often been used in drug design and development projects, with adenosine itself or its derivatives being used clinically since the 1940s.²

Extracellular adenosine is a signaling molecule that can activate adenosine receptors (ARs).² To this date four distinct and widely expressed human AR subtypes – A_1 , A_{2A} , A_{2B} and A_3 – have been discovered, each one implicated in a number of physiological and pathological processes. The structure, function, and basis for classification of ARs has been extensively reviewed.³ In particular, activation of ARs can induce inhibition (A_1 AR and A_3 AR) or activation (A_{2A} AR and A_{2B} AR) of adenylyl cyclase an enzyme that catalyses the conversion of ATP into cyclic adenosine monophosphate (cAMP). Activation or blockade of ARs is responsible for a wide range of effects in numerous organ systems and therefore the regulation of ARs can have many potential therapeutic applications.⁴ Pharmacological modulation of AR pathways open a new window for drug treatment of a variety of pathologies, such as asthma, neurodegenerative disorders, cancer, inflammatory and ischaemic related diseases.⁵⁻⁹

Coumarins are naturally occurring heterocyclic compounds with an in-depth history in Medicinal Chemistry,¹⁰ as they have been exploited in quite a lot of projects aiming to find, for instance, anti-cancer, antioxidant, anti-inflammatory, antimicrobial and antiviral agents.¹¹ Although benzopyran is considered a privileged structure, few studies have been addressed towards its application in the discovery of new ARs ligands. In this context, a number of coumarin based derivatives, in particular 3-aryl coumarins, have been reported by our group as inspiring ligands (**Figure 1**).¹²⁻¹⁵

Preliminary structure-activity relationship studies indicated that the nature of the substituents located in the coumarin ring, the presence or absence of a spacer between the pyrone ring and an aryl or alkyl side chain can modulate their affinity and selectivity, in particular towards A₃AR. To gain insight over the structural requirements needed for the development of a potent and selective AR coumarin-based ligand a series of 6-substituted coumarin derivatives was synthesised, characterised and pharmacologically evaluated. In addition, as amide group has also been proposed as operative either in coumarins or in chromones, a isomeric system, this type of spacer was chosen for the present study.¹⁶ The research was accomplished by receptor-driven molecular modelling studies.

Methods and materials

Materials and instruments

All starting materials and reagents were obtained from commercial suppliers and were used without further purification. Melting points (mp) were determined using a Reichert Kofler thermopan or a Büchi 510 apparatus and were not corrected. ¹H (250 MHz) and ¹³C (63 MHz) NMR spectra were recorded on a Bruker AMX spectrometer, using DMSO-*d*₆ or CDCl₃ as solvents. Chemical shifts (δ) and coupling constants (*J*) were expressed in ppm and in Hz, respectively. TMS was used as internal standard. The notations for multiplicity patterns were: s (singlet), d (doublet), dd (double doublet), t (triplet), dt (double triplet) and m (multiplet). Mass spectrometry data was acquired with a Hewlett-Packard-5972-MSD spectrometer. Silica gel (Merck 60, 230–400 mesh) was used for flash chromatography (FC). Analytical thin layer chromatography (TLC) was performed on plates precoated with silica gel (Merck 60 F254, 0.25 mm). Organic solutions were dried over anhydrous Na₂SO₄. The solvents were evaporated on a rotary evaporator (Büchi Rotavapor).

Synthesis

General procedure for the synthesis of coumarin 3-phenylcarboxamides (**8-19**):

To a solution of coumarin-3-carboxylic acid (**5**, **6** or **7**, 1.0 mmol) in dichloromethane (DCM, 5 mL) 1-ethyl-3-(3-dimethylaminopropyl)carbodiimide (EDC, 1.1 mmol) and 4-dimethylaminopyridine (DMAP, 1.1 mmol) were added. The mixture was kept in an argon flux at 0 °C for five minutes. Shortly after, the aromatic amine (1.0 mmol) with the pretended substitution pattern was added in small portions. The reaction mixture was stirred at room temperature for 4 hours. The obtained precipitate was filtered and purified by column chromatography (hexane/ethyl acetate 9:1) or by recrystallization with ethanol to give the desired compounds.

The synthesis of the precursors (**3-7**) and compounds (**9**, **12**, **15**, **21**, **24**, **27**, **30**, **36**, **39**, **42**, **45** and **51**) has been previously described.¹⁷

N-(2'-Hydroxyphenyl)coumarin-3-carboxamide (**8**) Yield: 54%; mp: 269-270 °C. ¹H NMR (DMSO-*d*₆) δ (ppm), *J* (Hz): 6.82-6.92 (m, 3H, H-8, H-4', H-5'), 7.46-7.57 (m, 2H, H-6, H-7), 7.76 (d, 1H, H-5, *J*=7.4), 8.04 (d, 1H, H-3', *J*=7.1), 8.39 (d, 1H, H-6', *J*=7.1), 9.05 (s, 1H, H-4), 10.23 (s, 1H, OH), 11.11 (s, 1H, NH). ¹³C NMR (DMSO-*d*₆) δ (ppm): 161.2, 154.1, 148.5, 146.8, 134.6, 130.6, 126.7, 125.4, 124.4, 120.0, 119.3, 118.8, 116.4, 114.7, 101.4, 98.2. MS *m/z* (%): 281 (M⁺, 81), 174 (38), 173 (100), 101 (40), 89 (34).

N-(2'-Hydroxyphenyl)-6-methoxycoumarin-3-carboxamide (**10**) Yield: 47%; mp: 232-233 °C. ¹H NMR (DMSO-*d*₆) δ (ppm), *J* (Hz): 3.80 (s, 3H, OCH₃), 6.75-6.82 (m, 1H, H-4'), 6.86-6.95 (m, 2H, H-3', H-5'), 7.33 (dd, 1H, H-7, *J*=2.9, 9.1), 7.46 (d, 1H, H-8, *J*=9.1), 7.58 (d, 1H, H-5, *J*=2.9), 8.36 (dd, 1H, H-6', *J*=1.3, 7.8), 8.96 (s, 1H, H-4), 10.17 (s, 1H, OH), 11.10 (s, 1H, NH). ¹³C NMR (DMSO-*d*₆) δ (ppm): 161.2, 158.9, 156.1, 148.6, 148.3, 146.7, 126.6, 124.4, 122.4, 120.0, 119.3, 119.7, 118.8, 117.4, 114.7, 111.9, 55.9. MS *m/z* (%): 312 (M⁺, 32), 311 (100), 204 (62), 203 (96), 119 (60), 65 (18).

N-(2'-Methylphenyl)coumarin-3-carboxamide (**11**) Yield: 56%; mp: 212-213 °C. ¹H NMR (CDCl₃) δ (ppm), *J* (Hz): 2.42 (s, 3H, CH₃), 7.10 (td, 1H, H-4', *J*=1.2, 7.4), 7.22-7.29 (m, 2H, H-7, H-8), 7.38-7.47 (m, 2H, H-6, H-5'), 7.67-7.77 (m, 2H, H-5, H-3'), 8.25 (d, 1H, H-6', *J*=8.2), 9.04 (s, 1H, H-4), 10.79 (s, 1H, NH). ¹³C NMR (CDCl₃) δ (ppm): 164.3, 158.2, 148.8, 148.8, 134.2, 130.3, 129.8, 128.4, 126.6, 125.3, 124.8, 121.7, 118.6, 116.6, 116.5, 99.9, 18.0. MS *m/z* (%): 279 (M⁺, 71), 261 (29), 173 (100), 106 (70), 101, (37), 89 (35), 77 (10), 63 (11).

N-(2'-Methylphenyl)-6-methoxycoumarin-3-carboxamide (**13**) Yield: 71%; mp: 186-187 °C. ¹H NMR (CDCl₃) δ (ppm), *J* (Hz): 2.39 (s, 3H, CH₃), 3.86 (s, 3H, OCH₃), 7.02- 7.12 (m, 2H, H-4', H-5'), 7.18- 7.25 (m, 2H, H-3', H-7), 7.27 (d, 1H, H-5, *J*=2.9), 7.36 (d, 1H, H-8, *J*=9.1), 8.22 (d, 1H, H-6', *J*=8.1), 8.96 (s, 1H, H-4), 10.82 (s, 1H, NH). ¹³C NMR (CDCl₃) δ (ppm): 162.1, 159.2, 158.8, 148.9, 136.0, 135.9, 130.3, 128.7, 126.5, 125.0, 122.7, 121.7, 118.9, 117.6, 115.5, 110.5, 55.8, 17.9. MS *m/z* (%): 309 (M⁺, 86), 291 (51), 281 (29), 203 (100), 119 (49), 106 (72), 77 (18), 65 (15).

N-(2'-Methoxyphenyl)coumarin-3-carboxamide (**14**) Yield: 64%; mp: 239-240 °C. ¹H NMR (CDCl₃) δ (ppm), *J* (Hz): 3.97 (s, 3H, OCH₃), 6.92-7.14 (m, 3H, H-8, H-3', H-6'), 7.41 (m, 2H, H-6, H-4'), 7.71 (m, 2H, H-7, H-5'), 8.54 (d, 1H, H-5, *J*=7.6), 9.00 (s, 1H, H-4), 11.28 (s, 1H, NH). ¹³C NMR (CDCl₃) δ (ppm): 172.1, 150.2, 148.4, 144.5, 140.9, 134.0, 129.7, 127.4, 125.2, 124.4, 120.8, 120.5, 118.3, 116.6, 111.0, 110.1, 55.9. MS *m/z* (%): 295 (M⁺, 79), 264 (27), 187 (10), 173 (100), 122 (17), 101 (30), 89 (23).

N-(2'-Methoxyphenyl)-6-methoxycoumarin-3-carboxamide (**16**) Yield: 78%; mp: 193-194 °C. ¹H NMR (CDCl₃) δ (ppm), *J* (Hz): 3.85, 3.94 (s, 6H, 2 x OCH₃), 6.91 (td, 1H, H-4', *J*=1.5, 7.9), 6.99 (dd, 1H, H-3', *J*=1.5, 7.9), 7.03- 7.12 (m, 2H, H-5, H-5'), 7.22 (dd, 1H, H-7, *J*=3.0, 9.1), 7.33 (d, 1H, H-8, *J*=9.1), 8.51 (dd, 1H, H-6', *J*=1.7, 7.5), 8.91 (s, 1H, H-4), 11.32 (s, 1H, NH). ¹³C NMR (CDCl₃) δ (ppm): 156.5, 149.0, 148.2, 134.5, 131.9, 127.5, 124.39, 122.5, 120.7, 120.4, 119.0, 118.9, 117.6, 110.5, 110.0, 106.8, 63.4, 55.8. MS *m/z* (%): 326 (M⁺, 30), 325 (82), 294 (28), 204 (30), 203 (100), 119 (53), 65 (18).

N-(2'-Chlorophenyl)coumarin-3-carboxamide (**17**) Yield: 68%; mp: 220-221 °C. ¹H NMR (CDCl₃) δ (ppm), *J* (Hz): 7.10 (dt, 1H, H-7, *J*=1.5, 7.7), 7.26-7.47 (m, 4H, H-6, H-4', H-5', H-6'), 7.67-7.76 (m, 2H, H-8, H-3'), 8.56 (dd, 1H, H-5, *J*=1.5, 8.7), 9.02 (s, 1H, H-4), 11.34 (s, 1H, NH). ¹³C NMR (CDCl₃) δ (ppm): 159.4, 154.4, 150.7, 149.0, 134.3, 129.8, 129.2, 127.3, 125.3, 125.1, 122.1, 118.4, 117.7, 116.6, 114.9, 99.9. MS *m/z* (%): 299 (M⁺, 37), 264 (100), 173 (99), 145 (9), 101 (51), 89 (47), 75 (13), 63 (22).

N-(2'-Chlorophenyl)-6-methylcoumarin-3-carboxamide (**18**) Yield: 61%; mp: 203-204 °C. ¹H NMR (DMSO-*d*₆) δ (ppm), *J* (Hz): 2.35 (s, 3H, CH₃), 7.14 (td, 1H, H-4', *J*=1.5, 6.2), 7.32-7.45 (m, 2H, H-8, H-5'), 7.50-7.60 (m, 2H, H-6, H-3'), 7.79 (s, 1H, H-5), 8.48 (dd, 1H, H-6', *J*=1.5, 6.8), 8.95 (s, 1H, H-4), 11.24 (s, 1H, NH). ¹³C NMR (DMSO-*d*₆) δ (ppm): 171.4, 168.9, 159.7, 152.5, 149.2, 136.3, 134.9,

130.2, 129.5, 128.0, 125.5, 121.8, 118.5, 118.0, 116.8, 115.6, 20.6. MS m/z (%): 313 (M^+ , 22), 279 (32), 278 (93), 187 (100), 115 (25), 103 (20), 77 (15).

N-(2'-Chlorophenyl)-6-methoxycoumarin-3-carboxamide (**19**) Yield: 73%; mp: 200-201 °C. ^1H NMR (DMSO- d_6) δ (ppm), J (Hz): 3.80 (s, 3H, OCH₃), 7.15 (td, 1H, H-4', $J=1.4, 7.8$), 7.31-7.42 (m, 2H, H-7, H-5'), 7.48 (d, 1H, H-8, $J=9.0$), 7.54 (dd, 1H, H-3', $J=1.3, 7.8$), 7.61 (d, 1H, H-5, $J=3.0$), 8.49 (dd, 1H, H-6', $J=1.4, 8.4$), 9.01 (s, 1H, H-4), 11.29 (s, 1H, NH). ^{13}C NMR (DMSO- d_6) δ (ppm): 166.6, 159.8, 156.2, 154.9, 149.0, 148.7, 138.0, 134.8, 129.6, 128.3, 128.1, 122.9, 121.5, 118.4, 117.8, 112.1, 56.0. MS m/z (%): 329 (M^+ , 45), 295 (54), 294 (99), 204 (37), 205 (100), 119 (60).

N-(2'-Bromophenyl)coumarin-3-carboxamide (**20**) Yield: 32%; mp: 218-219 °C. ^1H NMR (CDCl₃) δ (ppm), J (Hz): 7.04 (t, 1H, H-4', $J=7.6$), 7.33-7.47 (m, 3H, H-6, H-8, H-5'), 7.60-7.76 (m, 3H, H-5, H-7, H-3'), 8.51 (d, 1H, H-6', $J=8.0$), 9.01 (s, 1H, H-4), 11.21 (s, 1H, NH). ^{13}C NMR (CDCl₃) δ (ppm): 160.9, 160.0, 154.4, 149.1, 136.1, 134.4, 132.6, 129.8, 128.0, 125.6, 125.3, 122.7, 118.5, 118.4, 116.7, 114.4. MS m/z (%): 345 (M^+ , 25), 343 (24), 265 (58), 264 (99), 173 (100), 101 (59), 89 (66), 63 (33)

N-(2'-Bromophenyl)-6-methoxycoumarin-3-carboxamide (**22**) Yield: 36%; mp: 203-204 °C. ^1H NMR (DMSO- d_6) δ (ppm), J (Hz): 3.80 (s, 3H, OCH₃), 7.09 (td, 1H, H-4', $J=1.5, 8.0$), 7.33-7.45 (m, 2H, H-7, H-5'), 7.49 (d, 1H, H-8, $J=9.1$), 7.61 (d, 1H, H-5, $J=2.9$), 7.69 (dd, 1H, H-3', $J=1.4, 8.0$), 8.43 (dd, 1H, H-6', $J=1.5, 8.3$), 9.02 (s, 1H, H-4), 11.16 (s, 1H, NH). ^{13}C NMR (DMSO- d_6) δ (ppm): 171.9, 170.1, 166.9, 156.3, 149.1, 148.7, 148.0, 142.8, 136.6, 128.5, 124.4, 122.9, 122.6, 122.4, 117.6, 112.3, 56.0. MS m/z (%): 375 (M^+ , 16), 295 (44), 294 (98), 204 (23), 203 (100), 187 (55), 119 (24).

N-(3'-Hydroxyphenyl)coumarin-3-carboxamide (**23**) Yield: 51%; mp: 283-284 °C. ^1H NMR (DMSO- d_6) δ (ppm), J (Hz): 6.53 (dd, 1H, H-4', $J=2.0, 8.1$), 6.97-7.19 (m, 2H, H-8, H-5'), 7.31 (t, 1H, H-2', $J=2.0$), 7.41-7.58 (m, 2H, H-6, H-7), 7.72-7.80 (m, 1H, H-5), 8.00 (dd, 1H, H-6', $J=2.0, 7.8$), 8.88 (s, 1H, H-4), 9.55 (s, 1H, OH), 10.57 (s, 1H, NH). ^{13}C NMR (DMSO- d_6) δ (ppm): 161.3, 160.8, 156.7, 149.1, 147.0, 134.9, 129.9, 126.9, 125.1, 122.6, 119.8, 119.7, 119.0, 117.2, 114.1, 100.4. MS m/z (%): 281 (M^+ , 60), 253 (21), 173 (100), 101 (30), 89 (24).

N-(3'-Hydroxyphenyl)-6-methoxycoumarin-3-carboxamide (**25**) Yield: 57%; mp: 232-233 °C ¹H NMR (DMSO-*d*₆) δ (ppm), *J* (Hz): 3.80 (s, 3H, CH₃), 6.51 (dd, 1H, H-4', *J*=2.3, 8.0), 7.11 (t, 1H, H-5', *J*=8.0), 7.26-7.37 (m, 2H, H-7, H-6'), 7.48 (d, 1H, H-8, *J*=9.1), 7.55 (t, 1H, H-2', *J*=2.3), 8.83 (s, 1H, H-4), 9.55 (s, 1H, OH), 10.59 (s, 1H, NH). ¹³C NMR (DMSO-*d*₆) δ (ppm): 161.6, 160.0, 157.8, 153.1, 147.4, 130.0, 125.7, 122.5, 120.0, 117.6, 111.7, 110.9, 108.9, 107.0, 106.7, 104.4, 56.6. MS *m/z* (%): 312 (M⁺, 32), 311 (100), 204 (62), 203 (96), 119 (60), 80 (18).

N-(3'-Methylphenyl)coumarin-3-carboxamide (**26**) Yield: 34%; mp: 206-207 °C. ¹H NMR (CDCl₃) δ (ppm), *J* (Hz): 2.38 (s, 3H, CH₃), 6.98 (d, 1H, H-4', *J*=7.4), 7.24 (dd, 1H, H-5, *J*=1.3, 7.4), 7.38-7.46 (m, 2H, H-6, H-7), 7.50-7.59 (m, 2H, H-8, H-6'), 7.66-7.75 (m, 2H, H-2', H-5'), 9.02 (s, 1H, H-4), 10.79 (s, 1H, NH). ¹³C NMR (CDCl₃) δ (ppm): 161.1, 159.1, 154.3, 148.8, 138.8, 134.2, 129.8, 128.8, 125.5, 125.4, 121.4, 117.5, 116.6, 103.6, 101.6, 98.4, 21.4. MS *m/z* (%): 279 (M⁺, 75), 173 (100), 101 (29), 89 (24).

N-(3'-Methylphenyl)-6-methoxycoumarin-3-carboxamide (**28**) Yield: 73%; mp: 186-187 °C ¹H NMR (CDCl₃) δ (ppm), *J* (Hz): 2.34 (s, 3H, CH₃), 3.87 (s, 3H, OCH₃), 7.07 (d, 1H, H-5, *J*=2.9), 7.17-7.28 (m, 2H, H-2', H-5'), 7.34 (d, 1H, H-8, *J*=9.1), 7.47-7.55 (m, 2H, H-7, H-6'), 8.92 (s, 1H, H-4), 10.81 (s, 1H, NH). ¹³C NMR (CDCl₃) δ (ppm): 162.1, 159.2, 158.8, 148.6, 136.0, 135.9, 130.3, 128.8, 126.6, 125.0, 122.8, 121.7, 118.9, 117.7, 115.53, 110.52, 55.8, 18.0. MS *m/z* (%): 310 (M⁺, 22), 309 (86), 291 (51), 281 (30), 203 (100), 119 (49), 106 (72), 77 (17).

N-(3'-Methoxyphenyl)coumarin-3-carboxamide (**29**) Yield: 47%; mp: 189-190 °C. ¹H NMR (CDCl₃) δ (ppm), *J* (Hz): 3.85 (s, 3H, OCH₃), 6.70-6.76 (m, 1H, H-4'), 7.21-7.32 (m, 2H, H-8, H-2'), 7.38-7.52 (m, 3H, H-6, H-7, H-5'), 7.67-7.77 (m, 2H, H-5, H-6'), 9.02 (s, 1H, H-4), 10.85 (s, 1H, NH). ¹³C NMR (CDCl₃) δ (ppm): 161.6, 160.0, 159.1, 154.3, 148.8, 138.7, 134.2, 129.8, 129.6, 125.4, 118.6, 118.5, 116.6, 112.7, 110.8, 109.8, 55.2. MS *m/z* (%): 295 (M⁺, 68), 267 (35), 187 (10), 173 (100), 101 (32), 89 (21).

N-(3'-Methoxyphenyl)-6-methoxycoumarin-3-carboxamide (**31**) Yield: 67%; mp: 193-194 °C. ¹H NMR (CDCl₃) δ (ppm), *J* (Hz): 3.81, 3.85 (s, 6H, 2 x OCH₃), 6.68 (dt, 1H, H-4', *J*=2.2, 7.0), 7.06 (d, 1H, H-5, *J*=2.8), 7.18-7.28 (m, 3H, H-7, H-5', H-6'), 7.34 (d, 1H, H-8, *J*=9.1), 7.44 (t, 1H, H-2', *J*=2.2), 8.92 (s, 1H, H-4), 10.87 (s, 1H, NH). ¹³C NMR (CDCl₃) δ (ppm): 161.8, 160.0, 159.2, 156.6, 149.0, 148.6, 138.7,

129.6, 122.8, 118.9, 118.5, 117.7, 112.7, 110.7, 110.5, 105.8, 55.8, 55.2. MS m/z (%): 325 (M^+ , 53), 204 (100), 173 (94), 122 (30).

N-(3'-Chlorophenyl)coumarin-3-carboxamide (**32**) Yield: 60%; mp: 217-218 °C. ^1H NMR (DMSO- d_6) δ (ppm), J (Hz): 7.10 (dt, 1H, H-4', $J=1.5$, 7.8), 7.37-7.49 (m, 2H, H-6, H-8), 7.53-7.59 (m, 2H, H-7, H-5'), 7.78 (t, 1H, H-2', $J=1.5$), 7.96 (s, 1H, H-5), 8.01 (dd, 1H, H-6', $J=1.5$, 7.8), 8.89 (s, 1H, H-4), 10.74 (s, 1H, NH). ^{13}C NMR (DMSO- d_6) δ (ppm): 164.4, 160.9, 159.4, 147.7, 133.4, 132.7, 130.8, 130.5, 128.4, 125.5, 120.0, 119.6, 118.6, 116.4, 113.4, 101.0. MS m/z (%): 299 (M^+ , 67), 173 (100), 101 (36), 89 (30), 63 (13).

N-(3'-Chlorophenyl)-6-methylcoumarin-3-carboxamide (**33**) Yield: 61%; mp: 238-239 °C ^1H NMR (DMSO- d_6) δ (ppm), J (Hz): 2.36 (s, 1H, CH₃), 7.17 (dt, 1H, H-4', $J=1.8$, 8.0), 7.32-7.44 (m, 2H, H-8, H-5'), 7.50-7.60 (m, 2H, H-7, H-6'), 7.75 (d, 1H, H-5, $J=1.3$), 7.93 (t, 1H, H-2', $J=1.8$), 8.79 (s, 1H, H-4), 10.73 (s, 1H, NH). ^{13}C NMR (DMSO- d_6) δ (ppm): 174.7, 166.3, 160.5, 152.2, 149.2, 147.7, 135.5, 134.9, 133.4, 130.8, 129.9, 120.9, 119.6, 118.6, 118.2, 108.6, 20.4. MS m/z (%): 315 (M^+ , 60), 313 (M^+ , 93), 188 (77), 187 (100), 115 (70), 103 (63), 89 (16), 77 (53), 63 (19).

N-(3'-Chlorophenyl)-6-methoxycoumarin-3-carboxamide (**34**) Yield: 48%; mp: 222-223 °C ^1H NMR (DMSO- d_6) δ (ppm), J (Hz): 3.80 (s, 3H, OCH₃), 7.17 (dt, 1H, H-4', $J=1.9$, 7.8), 7.30-7.38 (m, 2H, H-5, H-7), 7.47 (d, 1H, H-8, $J=9.1$), 7.50-7.57 (m, 2H, H-5', H-6'), 7.94 (t, 1H, H-2', $J=1.9$), 8.83 (s, 1H, H-4), 10.76 (s, 1H, NH). ^{13}C NMR (DMSO- d_6) δ (ppm): 162.0, 160.5, 156.2, 149.3, 147.6, 139.5, 133.4, 130.8, 128.6, 127.7, 122.5, 119.6, 118.6, 117.6, 112.0, 103.6, 55.9. MS m/z (%): 331 (M^+ , 15), 329 (M^+ , 45), 295 (54), 294 (99), 204 (37), 203 (100), 119 (60).

N-(3'-Bromophenyl)coumarin-3-carboxamide (**35**) Yield: 33%; mp: 232-233 °C. ^1H NMR (CDCl₃) δ (ppm), J (Hz): 7.21 (d, 1H, H-8, $J=7.8$), 7.26-7.31 (m, 1H, H-7), 7.40-7.47 (m, 2H, H-6, H-5'), 7.62 (dt, 1H, H-6', $J=1.8$, 7.7), 7.68-7.76 (m, 2H, H-4', H-5), 8.03 (d, 1H, H-2', $J=1.8$), 9.02 (s, 1H, H-4), 10.88 (s, 1H, NH). ^{13}C NMR (CDCl₃) δ (ppm): 161.6, 160.9, 156.2, 154.4, 145.4, 144.0, 143.6, 141.2, 139.5, 138.8, 132.6, 129.9, 125.7, 125.5, 118.9, 106.1. MS m/z (%): 345 (M^+ , 58), 343 (M^+ , 58), 174 (36), 173 (100), 101 (46), 90 (17), 89 (51), 63 (30).

N-(3'-Bromophenyl)-6-methoxycoumarin-3-carboxamide (**37**) Yield: 53%; mp: 234-235 °C. ¹H NMR (DMSO-*d*₆) δ (ppm), *J* (Hz): 3.81 (s, 3H, OCH₃), 7.28-7.33 (m, 2H, H-5', H-7), 7.36 (d, 1H, H-5, *J*=3.0), 7.47 (d, 1H, H-8, *J*=9.0), 7.54-7.63 (m, 2H, H-4', H-6'), 8.07 (s, 1H, H-2'), 8.82 (s, 1H, H-4), 10.74 (s, 1H, NH). ¹³C NMR (DMSO-*d*₆) δ (ppm): 161.5, 160.6, 159.1, 155.0, 145.9, 145.2, 143.6, 141.2, 138.8, 132.6, 129.9, 125.7, 125.5, 120.7, 118.9, 101.4, 56.0. MS *m/z* (%): 375 (M⁺¹, 23), 374 (M⁺, 61), 203 (100), 187 (42), 119 (33).

N-(4'-Hydroxyphenyl)coumarin-3-carboxamide (**38**) Yield: 42%; mp: 261-262 °C. ¹H NMR (DMSO-*d*₆) δ (ppm), *J* (Hz): 6.75 (d, 2H, H-3', H-5', *J*=7.5), 7.41- 7.58 (m, 4H, H-7, H-8, H-2', H-6'), 7.76 (t, 1H, H-6, *J*=6.8), 8.01 (d, 1H, H-5, *J*=6.8), 8.89 (s, 1H, H-4), 9.37 (s, 1H, OH), 10.44 (s, 1H, NH). ¹³C NMR (DMSO-*d*₆) δ (ppm): 164.0, 161.0, 159.1, 152.0, 151.5, 144.2, 139.0, 135.1, 130.1, 126.4, 121.1, 120.3, 107.4. MS *m/z* (%): 281 (M⁺, 59), 173 (100), 101 (17), 89 (20)

N-(4'-Hydroxyphenyl)-6-methoxycoumarin-3-carboxamide (**40**) Yield: 59%; mp: 242-243 °C ¹H NMR (DMSO-*d*₆) δ (ppm), *J* (Hz): 3.80 (s, 3H, OCH₃), 7.23-7.60 (m, 5H, H-5, H-7, H-8, H-3', H-5'), 7.80 (d, 2H, H-2', H-6', *J*=8.4), 8.86 (s, 1H, H-4), 9.01 (s, 1H, OH), 10.76 (s, 1H, NH). ¹³C NMR (DMSO-*d*₆) δ (ppm): 161.2, 159.0, 156.2, 148.6, 148.3, 146.8, 126.6, 124.5, 122.5, 120.1, 119.3, 119.2, 118.9, 117.5, 114.7, 112.0, 56.0. MS *m/z* (%): 312 (M⁺, 21), 311 (86), 204 (22), 203 (100), 119 (23).

N-(4'-Methylphenyl)coumarin-3-carboxamide (**41**) Yield: 88%; mp: 236-237 °C ¹H NMR (CDCl₃) δ (ppm), *J* (Hz): 2.27 (s, 3H, CH₃), 7.17 (d, 2H, H-3', H-5', *J*=8.4), 7.45 (m, 1H, H-6), 7.53 (d, 1H, H-8, *J*=8.3), 7.59 (d, 2H, H-2', H-6', *J*=8.4), 7.75 (m, 1H, H-7), 7.99 (dd, 1H, H-5, *J*=1.7, 8.0), 8.89 (s, 1H, H-4), 10.57 (s, 1H, NH). ¹³C NMR (CDCl₃) δ (ppm): 160.4, 160.2, 159.8, 157.2, 147.5, 135.6, 134.4, 133.5, 130.4, 129.6, 122.5, 120.0, 118.7, 116.4, 20.6. MS *m/z* (%): 279 (M⁺, 54), 173 (100), 137 (53), 101 (19), 84 (21), 66 (22).

N-(4'-Methylphenyl)-6-methoxycoumarin-3-carboxamide (**43**) Yield: 61%; mp: 186-187 °C ¹H NMR (CDCl₃) δ (ppm), *J* (Hz): 2.24 (s, 3H, CH₃), 3.72 (s, 3H, OCH₃), 7.10-7.21 (m, 3H, H-5, H-2', H-6'), 7.41 (d, 1H, H-8, *J*=8.6), 7.52-7.61 (m, 3H, H-7, H-3', H-5'), 8.79 (s, 1H, H-4), 10.56 (s, 1H, NH). ¹³C NMR (CDCl₃)

δ (ppm): 162.1, 159.2, 158.8, 148.6, 136.0, 135.9, 130.3, 128.8, 126.6, 125.0, 122.8, 121.7, 118.9, 117.7, 115.5, 110.5, 55.80, 18.0. MS m/z (%): 309 (M^+ , 86), 291 (51), 281 (29), 203 (100), 119 (49), 106 (72).

N-(4'-Methoxyphenyl)coumarin-3-carboxamide (**44**) Yield: 74%; mp: 219-220 °C ^1H NMR (CDCl_3) δ (ppm), J (Hz): 3.96 (s, 3H, OCH_3), 6.96 (d, 2H, H-3', H-5', $J=8.3$), 7.32-7.43 (m, 2H, H-6, H-8), 7.59-7.66 (m, 3H, H-7, H-2', H-6'), 7.89 (m, 1H, H-5), 8.76 (s, 1H, H-4), 10.88 (s, 1H, NH). ^{13}C NMR (CDCl_3) δ (ppm): 163.7, 160.5, 159.9, 158.3, 146.1, 134.2, 134.0, 133.0, 131.4, 129.9, 120.5, 120.1, 118.7, 109.8, 55.9. MS m/z (%): 295 (M^+ , 66), 187 (22), 173 (100), 101 (43), 89 (18).

N-(4'-Methoxyphenyl)-6-methoxycoumarin-3-carboxamide (**46**) Yield: 59%; mp: 201-202 °C ^1H NMR (CDCl_3) δ (ppm), J (Hz): 3.80, 3.85 (s, 6H, 2 x OCH_3), 6.87-6.95 (m, 3H, H-5, H-3', H-5'), 7.29 (d, 1H, H-8, $J=9.0$), 7.44-7.58 (m, 3H, H-7, H-2', H-6'), 8.34 (s, 1H, H-4), 10.46 (s, 1H, NH). ^{13}C NMR (CDCl_3) δ (ppm): 162.9, 159.8, 159.3, 153.0, 148.6, 148.4, 130.1, 128.7, 120.0, 119.2, 118.4, 114.4, 112.4, 110.0, 105.1, 102.1, 55.8, 55.3. MS m/z (%): 325 (M^+ , 61), 203 (100), 173 (90), 108 (21).

N-(4'-Chlorophenyl)coumarin-3-carboxamide (**47**) Yield: 41%; mp: 264-265 °C ^1H NMR ($\text{DMSO-}d_6$) δ (ppm), J (Hz): 7.46 (d, 2H, H-3', H-5', $J=7.5$), 7.52-7.58 (m, 2H, H-6, H-8), 7.76 (d, 2H, H-2', H-6', $J=7.5$), 7.80-7.83 (m, 1H, H-7), 7.97 (d, 1H, H-5, $J=8.3$), 8.90 (s, 1H, H-4), 10.72 (s, 1H, NH). ^{13}C NMR ($\text{DMSO-}d_6$) δ (ppm): 163.1, 160.8, 159.2, 140.7, 139.7, 136.7, 132.7, 130.0, 129.4, 120.3, 119.7, 111.5, 110.9, 110.3, 102.0, 101.9. MS m/z (%): 301 ($M+2$, 28), 299 (M , 59), 173 (100), 101 (33), 89 (29), 63 (15).

N-(4'-Chlorophenyl)-6-methylcoumarin-3-carboxamide (**48**) Yield: 42%; mp: 216-217 °C ^1H NMR ($\text{DMSO-}d_6$) δ (ppm), J (Hz): 2.36 (s, 3H, CH_3), 7.35-7.45 (m, 3H, H-8, H-3', H-5'), 7.57 (dd, 1H, H-7, $J=2.0, 8.6$), 7.69-7.79 (m, 3H, H-5, H-2', H-6'), 8.79 (s, 1H, H-4), 10.70 (s, 1H, NH). ^{13}C NMR ($\text{DMSO-}d_6$) δ (ppm): 165.7, 160.3, 152.2, 147.7, 137.4, 135.53, 134.9, 132.1, 130.0, 122.0, 119.9, 118.6, 116.2, 107.8, 20.5 MS m/z (%): 315 (M^{+2} , 40), 313 (M^+ , 92), 188 (42), 187 (100), 115 (36), 103 (29), 77 (23).

N-(4'-Chlorophenyl)-6-methoxycoumarin-3-carboxamide (**49**) Yield: 49%; mp: 216-217 °C ^1H NMR ($\text{DMSO-}d_6$) δ (ppm), J (Hz): 3.80 (s, 3H, OCH_3), 7.28-7.40 (m, 2H, H-3', H-5'), 7.46 (d, 1H, H-8, $J=9.1$),

7.53 (d, 1H, H-5, $J=2.8$), 7.66-7.88 (m, 3H, H-7, H-2', H-6'), 8.82 (s, 1H, H-4), 10.71 (s, 1H, NH). ^{13}C NMR (DMSO- d_6) δ (ppm): 162.9, 160.9, 155.8, 149.1, 148.7, 139.5, 131.2, 131.1, 128.0, 126.3, 122.7, 119.1, 118.2, 117.8, 113.7, 100.4, 56.0. MS m/z (%): 329 (M^+ , 41), 295 (56), 294 (97), 204 (30), 203 (100), 119 (66), 76 (25).

N-(4'-Bromophenyl)coumarin-3-carboxamide (**50**) Yield: 34%; mp: 247-248 °C ^1H NMR (DMSO- d_6) δ (ppm), J (Hz): 7.44-7.49 (m, 1H, H-6), 7.52-7.57 (m, 3H, H-8, H-3', H-5'), 7.72 (d, 2H, H-2', H-6', $J=8.6$), 7.71-7.77 (m, 1H, H-7), 8.00 (dd, 1H, H-5, $J=1.5, 7.9$), 8.89 (s, 1H, H-4), 10.70 (s, 1H, NH). ^{13}C NMR (DMSO- d_6) δ (ppm): 168.6, 167.3, 148.0, 147.2, 145.4, 139.7, 136.2, 132.0, 129.7, 128.7, 117.4, 117.0, 111.1, 101.4. MS m/z (%): 345 (M^+ , 25), 343 (25), 173 (100), 101 (15), 89 (15).

N-(4'-Bromophenyl)-6-methoxycoumarin-3-carboxamide (**52**) Yield: 42%; mp: 269-270 °C ^1H NMR (DMSO- d_6) δ (ppm), J (Hz): 7.56-7.69 (m, 4H, H-7, H-8, H-3', H-5'), 7.72 (d, 2H, H-2', H-6', $J=8.4$), 7.78 (d, 1H, H-5, $J=1.2$), 8.64 (s, 1H, H-4), 10.49 (s, 1H, NH). ^{13}C NMR (DMSO- d_6) δ (ppm): 163.4, 161.2, 158.9, 148.8, 144.4, 140.0, 136.6, 130.1, 129.7, 129.5, 128.4, 117.8, 100.6, 99.6. MS m/z (%): 376 (M^{+2} , 27), 374 (69), 173 (100), 101 (22).

Pharmacology

The affinity of compounds **8–52** for the human AR subtypes hA_1 , hA_2A , hA_3 , was determined with radioligand competition experiments in Chinese hamster ovary (CHO) cells that were stably transfected with the individual receptor subtypes. The radioligands used were 1.0 nM (2R,3R,4S,5R)-2-(2-chloro-6-cyclopentylamino-purin-9-yl)-5-hydroxymethyl-tetrahydro-3,4-diol(^3H]CCPA) for hA_1 , 10.0 nM (1-(6-amino-9H-purin-9-yl)-1-deoxy-N-ethyl-b-D-ribofuronamide) (^3H]NECA) for hA_2A , and 1.0 nM 2-(1-hexynyl)- N^6 -methyladenosine [^3H] (^3H]HEMADO) for hA_3 receptors. The results were expressed as K_i values (dissociation constants), which were calculated with the program GraphPad. Due to the lack of a suitable radioligand for hA_2B receptors, the potency of antagonists at the hA_2B receptor (expressed on CHO cells) was determined by inhibition of NECA-stimulated adenylyl cyclase activity. The 50% inhibitory concentration (IC_{50}) for inhibition of cAMP (cyclic adenosine monophosphate) production was determined and converted to a K_i value using the Cheng and Prusoff equation. The K_i values (Table 1) are reported as geometric means of three independent experiments, with each tested concentration measured in duplicate. As an interval estimate for the

dissociation constants, 95% confidence intervals are given in parentheses. Details for pharmacological experiments are described in a previous work.¹⁴

Adenosine receptor homology models

Homology models of the hA_3 were previously developed by our group.^{15,16} Briefly, MOE software¹⁸ was used for the construction of the models and the hA_3 sequence was aligned to our template, the crystallized hA_{2A} AR (PDB code: 3EML).¹⁹ The alignment was based on previous studies related to adenosine homology modeling carried out by Katritch *et al.*²⁰ The geometry of the hA_3 model was assessed with the Protein Geometry module.¹⁸ Ability to discriminate ligands from decoys was also evaluated through ROC curves (area greater than 0.80).^{15,16,20} A more detailed description of the published homology models can be found in our previous studies.^{15,16,21}

Molecular docking

Molecular docking simulations in the hA_{2A} and the hA_3 were performed with Glide from the Schrödinger software.²² For the hA_3 docking the homology model previously described was used, whereas the crystal structure 3EML (PDB code)¹⁹ was used for the docking in the hA_{2A} . Protein structures were pre-processed with the Protein Preparation Wizard workflow included in Schrödinger.²² This process includes the assignment of bond orders, addition of cap termini, optimization of protonation states of the residues, and optimization of the hydrogen-bond protein network, among others. Ligands were prepared with the LigPrep module. No water molecules were included in the simulations. The compounds were docked to the proteins with Glide SP scoring function (standard precision).²² Binding modes described for graphical purposes were selected using parameters such as Emodel as well as number of similar poses generated through the calculations.

Theoretical evaluation of drug-like properties

The drug-like properties of the compounds under study were calculated using the Molinspiration property program. In this program, cLogP and topological polar surface area (TPSA) were calculated as a sum of fragment-based contributions and correction factors. The calculation of molecule volume has been performed by fitting the sum of fragment contributions to 'real' three dimensional (3D) volume for a training set of about 12 000 compounds, mostly drug-like molecules.²³

Results and discussion

Chemistry

Coumarin carboxamides **8-52** were efficiently synthesised following the strategy shown in Scheme 1. Generally, the compounds were obtained by an amidation reaction occurring between a coumarin-3-carboxylic acid (**5**, **6** and **7**) and the appropriate substituted amines using EDC as coupling reagent. Compounds **8-52** were obtained in moderate to high yields (32% to 88%). As only coumarin-3-carboxylic acid (**5**) was commercially available, 6-methylcoumarin-3-carboxylic (**6**) and 6-methoxycoumarin-3-carboxylic (**7**) acids were prepared by a Knoevenagel condensation of 5-methylsalicylaldehyde (**1**) and 5-methoxysalicylaldehyde (**2**), respectively, with diethyl malonate in ethanol using piperidine as catalyst and subsequent basic hydrolysis of the corresponding ester derivatives (compounds **3** and **4**, respectively). The overall reaction yield was 89% for the methyl substituted compound and 86% for its methoxy counterpart.

Pharmacology

The affinity of the coumarin carboxamides (compounds **8-52**) for the human AR subtypes hA_1 , hA_{2A} , hA_3 , which were expressed in Chinese hamster ovary (CHO) cells, was determined in radioligand competition experiments. In these assays, the competition with the following agonist radioligands: (i) [3 H]CCPA at hA_1 AR, (ii) [3 H]NECA at hA_{2A} and [3 H]HEMADO at hA_3 receptors was measured. The resulting binding affinity data expressed as K_i (dissociation constant) is reported in **Table 1**. The data regarding A_{2B} AR was not included as none of the tested compounds revealed a measurable affinity ($K_i > 30 \mu\text{M}$).

Structure-affinity relationship studies

In an effort for validate coumarin as a privileged structure for the design of AR ligands our research group acquired so far relevant data about scaffold recognized decorations (Figure 1). However, at the present step it was found important to perform a systematic study to attain a reliable structure-activity-relationship (SAR). Herein we present the first studies on coumarin decoration using carboxamide as a spacer and different substituents at position 6 of aromatic coumarin ring and at the exocyclic aromatic ring (**Figure 2**). The significance of the presence of a substituent at position 6 of the coumarin core was studied by the introduction of methyl or methoxy groups, as this position was denoted as relevant in some previous publications of our research group.^{14,15} In addition, the

effect our studies were focused on the effect of electron-donating and electron-withdrawing groups located at *ortho*, *meta* and *para* positions of the exocyclic aryl ring.

Generally, no relevant affinity data in any of ARs subtypes ($K_i > 100 \mu\text{M}$) was attained for the majority of the coumarin derivatives under study. However, it must be stressed that the results are of the utmost importance to improve our understanding on the effect of spacers and substituents on coumarin scaffold towards ARs subtypes. Accordingly, it can be concluded that the presence of electron-withdrawing substituents in the exocyclic aromatic ring (**17-22**, **32-37**, **47-52**, **Table 1**) have a negative outcome in the systems with absence or presence of substituents at the position 6 of coumarin ring.

In spite of these results, some interesting data was attained with electron-donating substituents allowing to draw some insights in the significance of 3-carboxamidocoumarin scaffold for the design of AR ligands. Although the introduction of a methoxy group in aromatic ring located on the side chain (**14-16**, **29-31**, **44-46**, **Table 1**), even in the presence or absence of substituents at the position 6 of coumarin ring substituents, was found to be not beneficial relevant data was attained by its replacement by methyl substituent (**11-13**, **26-38**, **41-43**, **Table 1**). In fact, compound **26** ($hA_3 K_i = 2.4 \mu\text{M}$) in which the group is located in *meta* position, display a noticeable activity and selectivity towards hA_3 , which is weakened if the group is moved for *ortho* (compound **13**, $hA_3 K_i = 45.4 \mu\text{M}$) or *para* position (compound **43**, $hA_3 K_i > 100 \mu\text{M}$). However, the affinity is dramatically reduced in the coumarins having methoxy or methyl substituents at the position 6.

For coumarins with a hydroxyl function in the exocyclic aromatic ring the data attained was not so ruled. Compound **8**, without any substituent in the coumarin core and a hydroxyl group located in *ortho* position, behave as a selective A_3 AR ligand ($hA_3 K_i = 31.5 \mu\text{M}$) Interestingly, it was noticed that the introduction of a methyl group at position 6 of the coumarin led to a loss of activity (compound **9**) whereas a methoxy group lead to a 30-fold decrease of the selectivity towards A_3 AR (compound **10**, $hA_1/hA_3 K_i = 1.21$). In the case of compounds **25** and **40**, with a hydroxyl group in the *meta* and *para* position and a methoxy at the position 6 of coumarin, respectively, a loss of selectivity was observed. Compound **25** has an A_1 AR binding affinity of $41 \mu\text{M}$ and a A_3 AR K_i of $22 \mu\text{M}$, while compound **40** has poor selectivity ($hA_1 K_i = 22.3 \mu\text{M}$, $hA_{2A} K_i = 28.3 \mu\text{M}$ and $hA_3 K_i = 24.2 \mu\text{M}$). The same tendency was observed for compounds **10** ($hA_1 K_i = 39.5 \mu\text{M}$, $hA_{2A} K_i = 38.0 \mu\text{M}$ and $hA_3 K_i = 32.7 \mu\text{M}$) and **38** ($hA_1 K_i > 30 \mu\text{M}$, $hA_{2A} K_i > 30 \mu\text{M}$ and $hA_3 K_i > 30 \mu\text{M}$).

Theoretical drug-like properties

To have a prediction of the drug-like properties of the most promising compounds some physicochemical parameters were calculated using the tool Molinspiration (**Table 2**).²³ These parameters include molecular weight (MW), number of heavy atoms (N), partition coefficient (clogP), topological polar surface area (tPSA in \AA^2), number of hydrogen bond acceptors (HBA), number of hydrogen bond donors (HBD), and number of rotatable bonds (n_{rotb}) and volume (\AA^3) (**Table 2**). For the coumarins under study no violation of Lipinski's rule of five (MW, log P, number of hydrogen donors and acceptors) were found. Moreover, the TPSA values, described as a predictive indicator of the drug capacity of membrane penetration, are encouraging for pursuing a drug-like lead. Consequently, the data represented in **Table 2** provides a preliminary indication that these type of compounds have drug-like properties.

Molecular docking simulations

Molecular docking simulations in the hA_{2A} and the hA_3 were carried out to study adenosine selectivity and provide some insights in the relationship between the molecular structure and the protein affinity. The crystal structure 3EML for the hA_{2A} and a homology model for the hA_3 were used in the simulations. Ligands were docked with Glide SP.²⁰ In previous studies¹⁵ our docking protocol was validated and a root mean square deviation (RMSD) of 0.69 and 1.92 between the co-crystallized and docking conformations for the ligands ZM241385 and T4E inside the hA_{2A} pocket was obtained.^{19,24}

Our studies have been initially focused on compound **26** as a significant selective binding affinity against the hA_3 ($K_i = 2.4 \mu\text{M}$, **Table 1**) has been attained. Molecular docking in the hA_3 yielded a pose for compound **26** in which the coumarin ring is oriented towards the bottom of the pocket whereas the 3'-methylphenyl group is located towards the extracellular area (see **Figure 3a**). The oxygen in the pyrone ring establishes a hydrogen bond with the amide group of the residue Asn250. Interactions with this residue have been already described in the literature for the different adenosine receptors.^{15,16,25} Moreover, the benzene ring in the coumarin nucleus of compound **26** establishes π - π stacking interactions with the residue Trp243. In addition, the contributions of the different residues to the binding of the ligand were also measured (see **Figure 3b**). The residue contribution score was calculated as the addition of *van der Waals* and Coulomb energies. The key contribution of some residues in the recognition of the ligand, such as Phe168, Leu246, Met177, Ile268, Trp243, Asn250 and Ala69 are shown in Figure 3b. However, other type of interactions, such

as hydrophobic interactions, could also be important to explain the different affinity between the compound and the protein. In fact, compound **26** placed the coumarin ring in a deep hydrophobic area and the 3'-methylphenyl is inserted also in a hydrophobic region (see **Figure 3a** with the hydrophobic/hydrophilic surface calculated in the hA_3 pocket).

The introduction of a hydroxyl group at ortho position of the phenyl group (compound **8**) lead to a dramatic decrease of the hA_3 binding affinity ($K_i = 31.5 \mu\text{M}$, Table 1), compared to compound **26**. The docking pose for compound **8** yielded a hydrogen bond with the residue Asn250 and π - π stacking interactions with the Phe168. A second hydrogen bond was detected between the 2'-hydroxyl group in the phenyl exocyclic ring and the residue Gln167 of the second extracellular loop (see **Figure 3c**). This fact could be a key factor to explain the hA_3 selectivity shown by compound **8**, since the other adenosine receptors do not present a glutamine residue (Gln) at the same position. However, the coumarin ring is placed in the hA_3 in a shallower hydrophobic region compared to compound **26** that could be responsible for the decrease of hA_3 activity. Docking studies have also been accomplished for compound **10** and from the pose extracted it was verified that the compound can establish a hydrogen bond with the residue Asn250 and π - π stacking interactions with the Phe168. Yet, the binding mode did not yield a hydrogen bond with the residue Gln167. However, the hydrophobic/hydrophilic surface of the receptor can accommodate the methoxy substituent in the hydrophobic area at the bottom of the cavity (see **Figure 3d**).

As compound **10** also exhibited a moderate affinity against hA_1 and hA_{2A} additional computational studies were performed. Since the crystal structure of hA_{2A} is available docking simulations were carried out to explain the increment in the affinity for hA_{2A} compared to the other compounds in the series. The simulations showed that compound **10** has a similar binding mode inside the hA_{2A} (see **Figure 4a**).

The ligand establishes a hydrogen bond with the residue Asn253. Moreover, π - π stacking interactions have been detected between the benzene ring in the coumarin nucleus and the imidazole of the residue His250. The 6-methoxy substituent was found to be well accommodated in a hydrophobic region, a pose that could be accountable for the observed increase on the hA_{2A} affinity compared to compounds **8** and **9**. Moreover, the 2'-hydroxyl substituent in the phenyl ring is oriented towards a hydrophilic area. The replacement in that position of a hydroxyl group by hydrophobic substituents, such as methyl or methoxy groups in compounds **13** and **16**, is not suitable for the interaction with the hA_{2A} with the consequent loss of affinity. Compound **26** showed a similar pose as compound **10**. However, the lack of the 6-methoxy substituent in the deep hydrophobic region along with the position of the 3'-methyl group of the phenyl ring in an area not

well defined as hydrophobic could be the reason for the decreased hA_{2A} affinity (see **Figure 4b**) of compounds **13** and **16**, is not be suitable for the interaction with the hA_{2A} with the consequent loss of affinity.

Conclusions

In this study, evidences for the validation of 3-phenylcarboxamidocoumarin as a scaffold for the development of AR ligands have been acquired. Due to coumarin synthetic accessibility and decoration capability a small library has been successfully attained and a concise SAR study performed. Although the majority of the compounds were not active for any of AR subtypes the data can be useful for validate the ligand requirements. In general, a loss of activity/selectivity was found for coumarins substituted in 6-position and with electron- withdrawing substituents in the aryl exocyclic ring. From the study interesting remarks must be highlighted: compound **26** displayed a relevant affinity and selectivity for hA_3 ($K_i = 2.4 \mu\text{M}$), turning it in the most stimulating compound of the series. Its hA_3 selectivity was elucidated by docking experiments that indicate that the coumarin ring is oriented towards the bottom of the pocket whereas the 3'-methylphenyl group is located towards the extracellular area and that the oxygen in the pyrone ring establishes a hydrogen bond with the amide group of the residue Asn250.

Taking into account that A_1 and A_3 AR ligands are beneficial for the treatment of disorders of the nervous system, such as chronic pain, neurodegeneration and brain injury, compound **26** can be considered an interesting starting point for further studies aiming the development of effective and selective coumarin-based AR ligands.

In summary, the data suggests that for this type of compounds the presence of substituents at position 6 can be detrimental for the AR affinity constituting per se an important tool for building upon the coumarin hits.

Acknowledgments

The authors would like to thank Fundação para a Ciência e Tecnologia (FCT) – QUI/UI0081/2013, POCI-01-0145-FEDER-006980 for the financial support. Thanks are due to FCT, POPH and QREN for A. Fonseca (SFRH/BD/80831/2011) and M. J. Matos (SFRH/BPD/95345/2013) doctoral and post-doctoral grants. S. Vilar also thanks “Angeles Alvariño program, Plan Galego de Investigación, Innovación e Crecemento 2011-2015 (I2C)” and “European Social Fund (ESF)”.

Conflict of interest

Authors declare no conflict of interest.

Figure 1. General structure of coumarin based derivatives described as AR ligands.^{12–15}

Figure 2. Rational design followed in the present study.

Figure 3. a) Hypothetical binding mode extracted from molecular docking for compound **26** in the hA_3 . Hydrogen bond with the residue Asn250 is shown in yellow dashes. Hydrophobic areas in the pocket are represented in yellow and hydrophilic regions in red color. b) Residue contributions to the binding between hA_3 and compound **26** (sum of *van der Waals* and Coulomb energies). c) Pose extracted for compound **8** in the hA_3 . Hydrogen bonds with the residues Asn250 and Gln167 are shown in yellow dashes. d) Hypothetical binding mode calculated for compound **10** in the hA_3 (hydrophobic surface in yellow and hydrophilic in red color).

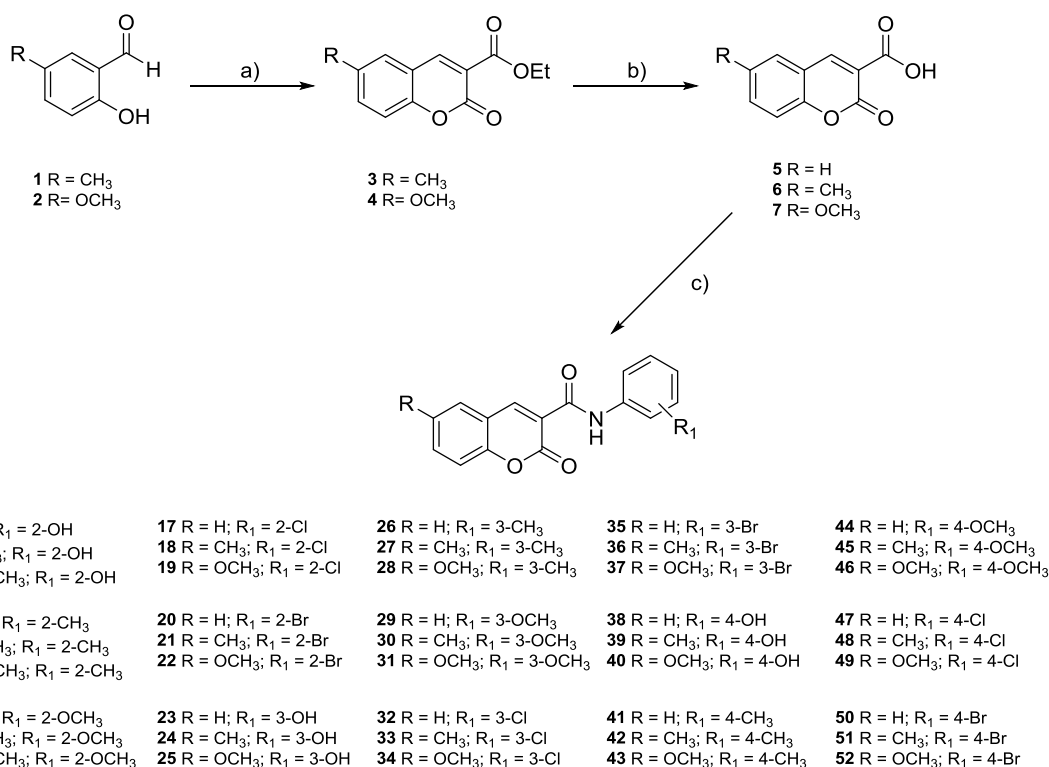
Figure 4. a) Hypothetical binding mode calculated with molecular docking for compound **10** in the hA_{2A} . Hydrogen bonds are represented in yellow dashes, hydrophobic surface in green color and hydrophilic surface in magenta. b) Pose calculated with docking for the compound **26** in the hA_{2A} .

References

1. Drury, N.; Szent-Györgyi, J. *Physiol.* **1929**, *68*, 213–237.
2. Chen, J. F.; Eltzhig, H. K.; Fredholm, B. B. *Nat. Rev. Drug Discov.* **2013**, *12*, 265–286.
3. Fredholm, B. B.; Jzerman, A. P.; Jacobson, K. A.; Klotz, K.-N.; Linden, J. *Pharmacol. Rev.* **2001**, *53*, 527–552.
4. Bours, M. J. L.; Swennen, E. L. R.; Di Virgilio, F.; Cronstein, B. N.; Dagnelie, P. C. *Pharmacol. Ther.* **2006**, *112*, 358–404.
5. Fredholm, B. B. *Exp. Cell Res.* **2010**, *316*, 1284–1288.

6. Gessi, S.; Cattabriga, E.; Avitabile, A.; Gafa, R.; Lanza, G.; Cavazzini, L.; Bianchi, N.; Gambari, R.; Feo, C.; Liboni, A.; Gullini, S.; Leung, E.; Mac-Lennan, S.; Borea, P. A. *Clin. Cancer Res.* **2004**, *10*, 5895–5901.
7. Jacobson, K. A.; Gao, Z. *Nat. Rev. Drug Discov.* **2006**, *5*, 247–264.
8. Fonslow, B. R.; Stein, B. D.; Webb, K. J.; Xu, T.; Choi, J.; Kyu, S.; Iii, J. R. Y. **2013**, *10*, 54–56.
9. Press, N. J.; Fozard, J. R. *Expert Opin. Ther. Pat.* **2010**, *20*, 987–1005.
10. Borges, F.; Roleira, F.; Milhazes, N.; Santana, L.; Uriarte, E. *Curr. Med. Chem.* **2005**, *12*, 887–916.
11. Borges, F.; Roleira, F. M. F.; Milhazes, N. J. da S. P.; Uriarte, E.; Santana, L. *Front. Med. Chem.* **2009**, *4*, 23–85.
12. Matos, M. J.; Vilar, S.; Kachler, S.; Celeiro, M.; Vazquez-Rodriguez, S.; Santana, L.; Uriarte, E.; Hripcsak, G.; Borges, F.; Klotz, K.-N. *Bioorg. Chem.* **2015**, *61*, 1–6.
13. Vazquez-Rodriguez, S.; Matos, M. J.; Santana, L.; Uriarte, E.; Borges, F.; Kachler, S.; Klotz, K. N. *J. Pharm. Pharmacol.* **2013**, *65*, 697–703.
14. Matos, M. J.; Hogger, V.; Gaspar, A.; Kachler, S.; Borges, F.; Uriarte, E.; Santana, L.; Klotz, K.-N. *J. Pharm. Pharmacol.* **2013**, *65*, 1590–1597.
15. Matos, M. J.; Vilar, S.; Kachler, S.; Fonseca, A.; Santana, L.; Uriarte, E.; Borges, F.; Tatonetti, N. P.; Klotz, K.-N. *ChemMedChem* **2014**, *9*, 2245–2253.
16. Cagide, F.; Gaspar, A.; Reis, J.; Chavarria, D.; Vilar, S.; Hripcsak, G.; Uriarte, E.; Kachler, S.; Klotz, K. N.; Borges, F. *RSC Adv.* **2015**, *5*, 78572–78585.
17. Fonseca, A.; Matos, M. J.; Reis, J.; Duarte, Y.; Santana, L.; Uriarte, E.; Borges, F. *RSC Adv.* **2016**, *6*, 49764–49768.
18. MOE, version 2011.10; Chemical Computing Group, Inc.: Available at: <http://www.chemcomp.com>. (Accessed: Jan 2012).
19. Veli-Pekka, J.; Mark, G.; Michael, H.; Vadim, C.; Ellen, Y.; Robert, L.; Adriaan, P. I.; Raymond, C. S. *Science.* **2008**, *322*, 1211–1217.
20. Katritch, V.; Kufareva, I.; Abagyan, R. *Neuropharmacology* **2011**, *60*, 108–115.

21. Matos, M. J.; Vilar, S.; Kachler, S.; Vazquez-Rodriguez, S.; Varela, C.; Delogu, G.; Hripcsak, G.; Santana, L.; Uriarte, E.; Klotz, K.-N.; Borges, F. *Med. Chem. Commun.* **2016**, *7*, 845–852.
22. Schrödinger suite 2016-3, Schrödinger, LLC, New York, USA, 2016. Available at: <http://www.schrodinger.com/> (Accessed: August 2016).
23. Lipinski, C.; Lombardo, F.; Dominy, B. W.; Feeney, P. J. *Adv. Drug Deliv. Rev.* **2012**, *64*, 4–17.
24. Congreve, M.; Andrews, S. P.; Doré, A. S.; Hollenstein, K.; Hurrell, E.; Langmead, C. J.; Mason, J. S.; Ng, I. W.; Tehan, B.; Zhukov, A.; Weir, M.; Marshall, F. H. *J. Med. Chem.* **2012**, *55*, 1898–1903.
25. Kolb, P.; Phan, K.; Gao, Z. G.; Marko, A. C.; Sali, A.; Jacobson, K. A. *PLoS One* **2012**, *7*, e49910.
26. Klotz, K.-N.; Hessling, J.; Hegler, J.; Owman, C.; Kull, B.; Fredholm, B. B.; Lohse, M. J. *Naunyn. Schmiedebergs. Arch. Pharmacol.* **1997**, *357*, 1–9.



Scheme 1. Synthetic strategy followed for the preparation of coumarin 3-phenylcarboxamides. Reagents and conditions: a) diethyl malonate, EtOH, piperidine, reflux, overnight. b) NaOH (0.5% aq./EtOH), reflux, 2 h. c) EDC, DMAP, DCM, corresponding amine, 0 °C to r.t., 4 h

Table 1. Binding affinity (K_i in μM and 95% confidence intervals in parentheses) of coumarins **8-52** in radioligand binding assays at human A_1 , A_{2A} , A_3 AR subtypes.

Compound	R	R_1	hA_1 K_i (μM)	hA_{2A} K_i (μM)	hA_3 K_i (μM)	Selectivity	
						hA_1/hA_3	hA_{2A}/hA_3
8	H	2-OH	> 100	> 30	31.5 (2.39 – 4.16)	>3.17	>0.95
9 ¹⁷	CH ₃	2-OH	> 100	> 100	> 30	–	–
10	OCH ₃	2-OH	39.5 (34.3 – 45.4)	38.0 (34.5 – 41.9)	32.7 (27.6 – 38.8)	1.21	1.16
11	H	2-CH ₃	> 100	> 100	> 100	–	–
12 ¹⁷	CH ₃	2-CH ₃	> 100	> 100	> 100	–	–
13	OCH ₃	2-CH ₃	> 100	> 100	45.4 (38.7 – 53.3)	>2.20	>2.20
14	H	2-OCH ₃	> 100	> 100	> 100	–	–
15 ¹⁷	CH ₃	2-OCH ₃	> 100	> 100	> 100	–	–
16	OCH ₃	2-OCH ₃	> 100	> 100	> 100	–	–
17	H	2-Cl	> 100	> 100	> 100	–	–
18	CH ₃	2-Cl	> 100	> 100	> 100	–	–
19	OCH ₃	2-Cl	> 100	> 100	> 100	–	–
20	H	2-Br	> 100	> 100	> 100	–	–
21 ¹⁷	CH ₃	2-Br	> 100	> 100	> 100	–	–
22	OCH ₃	2-Br	> 100	> 100	> 100	–	–
23	H	3-OH	> 100	> 100	> 100	–	–
24 ¹⁷	CH ₃	3-OH	> 100	> 100	> 100	–	–
25	OCH ₃	3-OH	41.0 (29.0 – 58.1)	> 100	22.0 (15.3 – 31.7)	1.86	>4.54
26	H	3-CH ₃	> 100	> 100	2.4 (1.81 – 3.19)	>41.67	>41.67
27 ¹⁷	CH ₃	3-CH ₃	> 100	> 100	> 100	–	–

28	OCH ₃	3-CH ₃	> 100	> 100	> 100	-	-
29	H	3-OCH ₃	> 100	> 100	> 100	-	-
30 ¹⁷	CH ₃	3-OCH ₃	> 100	> 100	> 100	-	-
31	OCH ₃	3-OCH ₃	> 100	> 100	> 100	-	-
32	H	3-Cl	> 30	> 30	> 30	-	-
33	CH ₃	3-Cl	> 30	> 30	> 30	-	-
34	OCH ₃	3-Cl	> 100	> 100	> 100	-	-
35	H	3-Br	> 30	> 30	> 100	-	-
36 ¹⁷	CH ₃	3-Br	> 10	> 10	> 10	-	-
37	OCH ₃	3-Br	> 100	> 100	> 100	-	-
38	H	4-OH	> 30	> 30	> 30	-	-
39 ¹⁷	CH ₃	4-OH	> 100	> 100	> 100	-	-
40	OCH ₃	4-OH	22.3 (21.5 – 23.2)	28.3 (25.2 – 31.8)	24.2 (22.2 – 26.4)	0.79	1.17
41	H	4-CH ₃	> 100	> 100	> 100	-	-
42 ¹⁷	CH ₃	4-CH ₃	> 100	> 100	> 100	-	-
43	OCH ₃	4-CH ₃	> 100	> 100	> 100	-	-
44	H	4-OCH ₃	> 100	> 100	> 100	-	-
45 ¹⁷	CH ₃	4-OCH ₃	> 100	> 100	> 100	-	-
46	OCH ₃	4-OCH ₃	> 100	> 100	> 100	-	-
47	H	4-Cl	> 100	> 100	> 100	-	-
48	CH ₃	4-Cl	> 100	> 100	> 100	-	-
49	OCH ₃	4-Cl	> 100	> 100	> 100	-	-
50	H	4-Br	> 30	> 30	> 30	-	-
51 ¹⁷	CH ₃	4-Br	> 100	> 100	> 100	-	-
52	OCH ₃	4-Br	> 100	> 100	> 100	-	-
theophylline ²⁶			6.77 (4.07 - 11.30)	-	86.40 (73.60 – 101.30)	0.08	1.2

Table 2. Drug-like properties of the most promising coumarins.

Compd	MW	N	clogP	tPSA (Å ²)	HBA	HBD	n _{rotb}	Vol (Å ³)
8	281.27	21	2.56	79.54	5	2	3	239.4
10	311.29	23	2.60	88.77	6	2	4	264.9
13	295.29	22	2.84	68.54	5	1	4	256.9
25	311.29	23	2.36	88.77	6	2	3	264.94
26	279.30	21	3.26	59.31	4	1	2	247.94
40	311.29	23	2.39	88.77	6	2	3	264.94

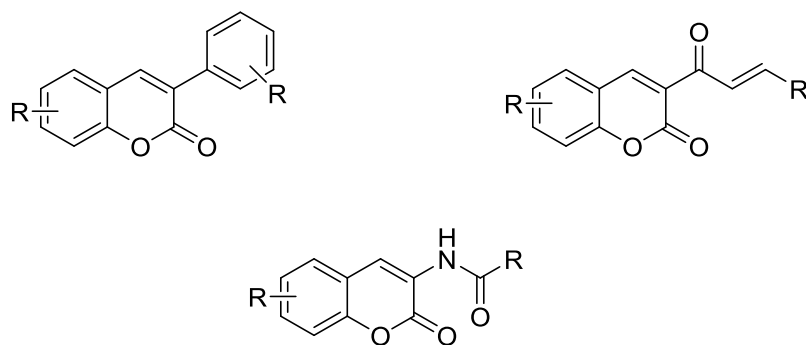


Figure 1. General structure of coumarin based derivatives described as AR ligands.^{12–15}

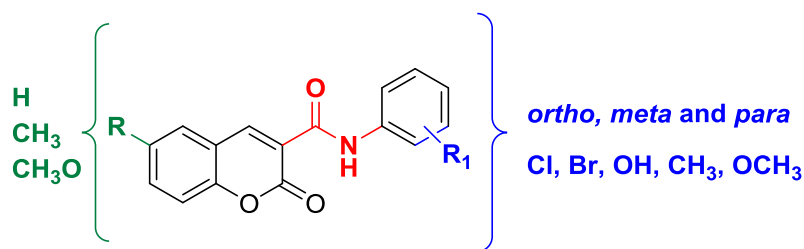


Figure 2. Rational design followed in the present study.

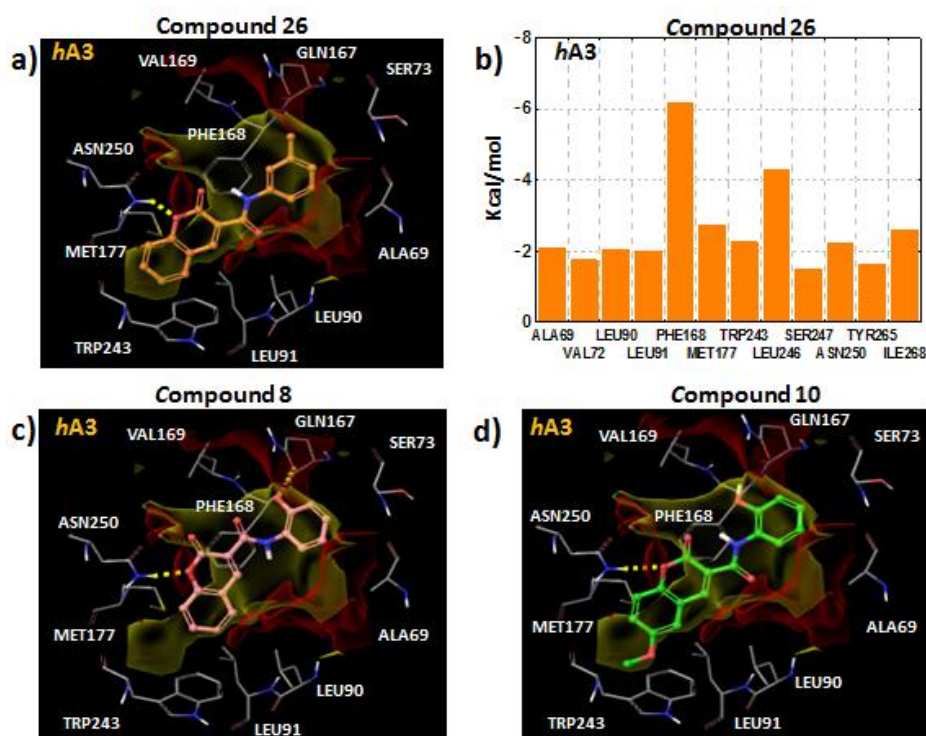


Figure 3. a) Hypothetical binding mode extracted from molecular docking for compound **26** in the hA_3 . Hydrogen bond with the residue Asn250 is shown in yellow dashes. Hydrophobic areas in the pocket are represented in yellow and hydrophilic regions in red color. b) Residue contributions to the binding between hA_3 and compound **26** (sum of *van der Waals* and Coulomb energies). c) Pose extracted for compound **8** in the hA_3 . Hydrogen bonds with the residues Asn250 and Gln167 are shown in yellow dashes. d) Hypothetical binding mode calculated for compound **10** in the hA_3 (hydrophobic surface in yellow and hydrophilic in red color).

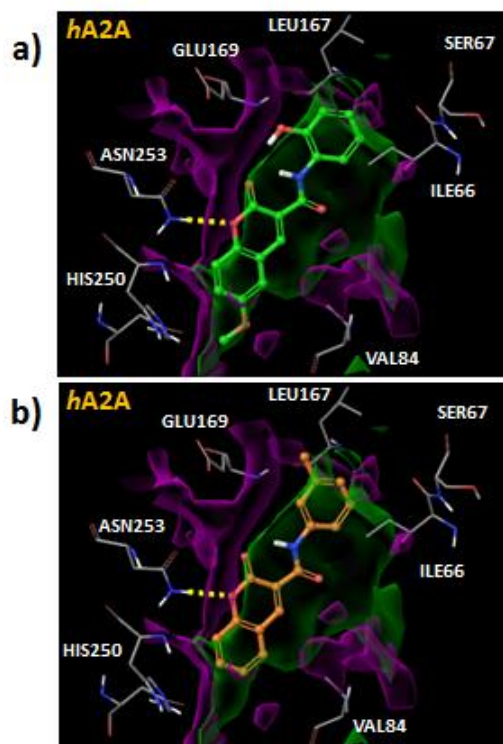


Figure 4. a) Hypothetical binding mode calculated with molecular docking for compound **10** in the *hA_{2A}*. Hydrogen bonds are represented in yellow dashes, hydrophobic surface in green color and hydrophilic surface in magenta. b) Pose calculated with docking for the compound **26** in the *hA_{2A}*.